PHYSICAL REVIEW A **93**, 021405(R) (2016)

Active tailoring of nanoantenna plasmonic fields using few-cycle laser pulses

S. Choi,[1,2] M. F. Ciappina,[3,*] J. A. Pérez-Hernández,[4] A. S. Landsman,[1,5] Y.-J. Kim,[6] S. C. Kim,[1,2,†] and D. Kim[1,2]

[1]*Max-Planck-Center for Attosecond Science (MPC-AS), Max Planck POSTECH/KOREA Res. Init., Pohang, Gyeongbuk 376-73, South Korea*

[2]*Center for Attosecond Science and Technology (CASTECH), POSTECH, Pohang, Gyeongbuk 376-73, South Korea*

[3]*Max-Planck Institut für Quantenoptik, Hans-Kopfermann-Straße 1, D-85748 Garching, Germany*

[4]*Centro de Láseres Pulsados (CLPU), Parque Científico, E-37008 Villamayor, Salamanca, Spain*

[5]*Max-Planck Institut für Physik komplexer Systeme, Nöthnitzer Straße 38, D-01187 Dresden, Germany*

[6]*School of Mechanical and Aerospace Engineering, Nanyang Technological University (NTU), 50 Nanyang Avenue, Singapore 639798, Singapore*

(Received 10 September 2015; revised manuscript received 19 January 2016; published 24 February 2016)

Plasmonic nanoatennas are a versatile tool for coherently manipulating light on a nanoscale by confining electric fields of the driving laser into subwavelength volumes, thereby significantly enhancing electric near fields. It is normally assumed that the time-dependent spectral properties of these near fields are independent of the duration of the driving laser pulse. Here we show that when a few-cycle laser pulse shines on a bow-tie nanoantenna, its spectral properties are dramatically modified, as evidenced by a large shift of the center wavelength of the near field, relative to the driving laser. In addition, for certain geometries, a second color appears in the near field, creating conditions for generation of an isolated attosecond pulse at megahertz repetition rate. Our results open the door to frequency-tunable ultrafast sources at nanometer scale without tuning the frequency of the driving laser.

DOI: 10.1103/PhysRevA.93.021405

The past decades have seen a considerable development in synthesis and fabrication methods of plasmonic nanostructures. This, in turn, led to active efforts to exploit their unique and unusual optical properties, which arise when light interacts with the resonant localized surface-plasmon modes [1–7]. A key feature of this light-nanostructure interaction is the enhancement of the resultant electric field by several orders of magnitude at metal-dielectric interfaces, and the local confinement of electric field on a subwavelength scale. Due to the particular coupling property from a propagating field into a localized field, a metallic nanoantenna has become an important tool for observing nano- and microscale optical responses of atoms and molecules, as used in surface enhanced Raman spectroscopy [8], quantum (optical) information processing, or enhancing the intensity of light emission [9,10]. Because of the strong-field enhancement, combined with a field localization, the interaction of plasmonic nanostructures with ultrashort laser pulses also provides a unique perspective on strong-field phenomena [11,12], such as high-order harmonic generation (HHG), which until recently [13–15] has only been investigated in spatially homogeneous electric fields of the driving laser.

It is well known that the spatial distribution of the near fields and the degree of enhancement is determined by the geometric properties of the nanoantenna. However, the effect of nanoantenna geometry on the spectral time-dependent properties of the near field, such as the central frequency, is less understood. In particular, it is typically assumed that these spectral properties are independent of the duration of the driving laser pulse. Since the HHG spectrum is highly sensitive to the temporal details of the localized field (in particular, the HHG cutoff scales as λ^2, where λ is the central wavelength of the driving laser field), it is critical to understand how the λ of the incident laser pulse is modified by the plasmonic structure. Although a recent study measured third harmonic yield and two-photon photoluminescence under excitation of a nanoantenna by a few-cycle pulse [16,17], the modification in the λ of the near field (relative to the laser field) has not been explored. Other studies have investigated experimentally the near field created by a femtosecond laser by measuring the extinction spectra [6,18]. However, these investigations used a many-cycle driving pulse, on the order of 30–100 fs, where the shift in λ was observed to be small.

In this Rapid Communication, we demonstrate that the spectral features in general, and the central wavelength of the localized ultrafast plasmonic field in particular, can be modified substantially under excitation by a few-cycle pulse. The degree and type of modification depends on the overlap between the frequency of the resonant mode of the dipole nanoantenna and the spectral bandwidth of the incident pulse. When these spectral specifications (components) are not well matched (intersected), resultant near field experiences a significant spectral shift with respect to the spectrum of the incident pulse. Note that this spectral shift depends not only on the geometry of the nanostructure and the λ of the driving laser, but also on pulse duration: the shift is pronounced for few-cycle pulses and becomes negligible for longer pulses. This new phenomenon can be exploited in the field of ultrafast nanoplasmonics to generate second and third harmonics at a nanoscale with a tunable λ by simply varying the duration of the driving laser pulse. Moreover, as we show, under certain conditions, it is possible to generate a near field favorable to the generation of an isolated attosecond pulse at megahertz repetition rate. We explain the physical reason for this attosecond pulse creation as resulting from substantial spectral modifications that lead to a significant shift in λ as well as an appearance of a second color in the near-field spectrum when a few-cycle driving laser is used.

As illustrated in Fig. 1(a), the bow-tie nanoantenna is characterized by four geometrical parameters: the thickness

*marcelo.ciappina@mpq.mpg.de
†inter99@postech.ac.kr

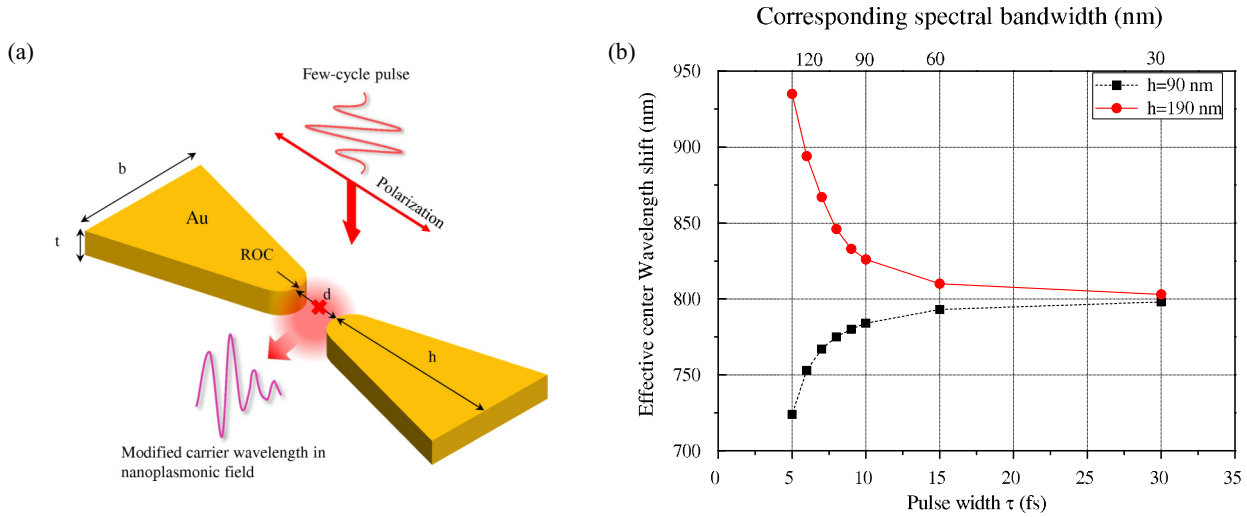

FIG. 1. (a) Geometrical parameters of bow-tie nanoantenna: h = height, b = bottom length, t = thickness, d = gap, and ROC = Radius of curvature. Data is collected at the middle of the bow-tie gap denoted as a red cross. Laser pulse is illuminated normal to the surface with polarization parallel to the bow-tie height. (b) Effective center wavelength shift of plasmonic near field for various pulse durations. Opposite directions of center wavelength shift were observed for two bow-tie heights (h = 90 and 190 nm), namely, redshift for the height of 190 nm (red circles) and blueshift for the height of 90 nm (black squares), respectively.

(t), bottom length (b), gap (d), and height (h) of the antenna. The radius of curvature (ROC) of 10 nm at the tip was used for all geometries, considering the possibility of fabrication. When light is illuminated on a nanoantenna, the near field at frequency ω is represented as $E_{\mathrm{loc},i}(\omega,\mathbf{r}_n) = \sum_j L_{i,j}(\omega,\mathbf{r}_n)E_j(\omega_n)$, where i and j stand for the Cartesian components of the electric field. The tensorial local field factor, $L_{i,j}(\omega,\mathbf{r}_n)$, can significantly modify the local field distribution when the surface plasmon is excited [2]. For sufficiently broadband excitation (corresponding to few cycles or less), and depending on the geometry, the local electric field spectral components may be modified substantially from that of the driving field. This happens whenever the resonance of the nanostructure is mismatched with the λ of the laser pulse, but overlaps significantly with the bandwidth. Hence the shift in the λ can be substantial and highly sensitive to nanoantenna geometry for a few-cycle pulse, but becomes negligible for longer pulses [see Fig. 1(b)].

The electromagnetic field around the nanoantenna was numerically calculated by using the commercial software LUMERICAL that implements the finite-difference time-domain (FDTD) method. The polarization direction of the incident femtosecond pulse was positioned parallel to the height direction as denoted in Fig. 1(a). In the simulation, the bandwidth of the incident pulse was predefined by its pulse width and λ was set at 800 nm. The nanoantenna is made of gold, whose wavelength-dependent complex dielectric constants were taken from Palik data [19].

Through iterative FDTD calculations, we found that the height (h) was the most sensitive parameter for determining the effective λ. As shown in Fig. 1(b), the heights of 190 and 90 nm were chosen to study the dependence of the resonance on spectral bandwidth because the large wavelength shift affects the spectrum of the dipole radiation in the gap. For all the data sets, t = 50 nm, b = 50 nm, and g = 20 nm were used. The induced field was extracted at the center of a bow-tie gap (see the red cross in Fig. 1(a)). Figure 1(b) shows the shift of the center wavelength for different pulse durations. The black-dashed line represents the shift of λ for h = 90 nm and the red-solid line for h = 190 nm as a function of pulse width (τ) ranging from 5 to 30 fs (this is equivalent to changing the bandwidth of a transform-limited pulse). For τ = 5 fs, the distinct shift of λ corresponds to 720 nm in the blue end and 935 nm in the red end for the given bow-tie heights of 90 and 190 nm, respectively.

This significant shift of λ, that can be controlled by bow-tie geometry, is particularly important in the study of nonlinear light emission, such as HHG, and should therefore be considered whenever few-cycle pulses are used (Note that for longer pulses, the bow-tie geometry only determines the magnitude of the field enhancement). Hence the bow-tie geometry influences not only the magnitude of field enhancement but also the spectral distribution of the resultant near field when a sufficiently broadband light pulse is used. To characterize this effect, we calculated the inherent resonance behavior of each plasmonic nanoantenna for different wavelengths of light excitation. By sweeping the wavelength of a single wavelength (SW) source, the resonance condition of each nanoantenna was obtained. The resonance wavelength of the nanoantenna is defined as the wavelength where maximum field enhancement and spectral power at the gap of the nanoantenna is generated. Four heights were specified for these calculations: h = 90, 190, 350, and 450 nm. The cases of h = 90 and 190 nm represent the bow-tie structures that show large λ shifts in opposite directions and can therefore be used to blue- or redshift the driving laser light, respectively. The other two cases of h = 350 and 450 nm show major and minor resonance peaks for sufficiently short laser pulses, which, as we show, are advantageous for the generation of isolated attosecond pulses via HHG.

SW excitation sources were varied from 500 to 1100 nm in wavelength with a step of ∼5 nm. The results are shown in Fig. 2. We find that the intrinsic resonance wavelengths

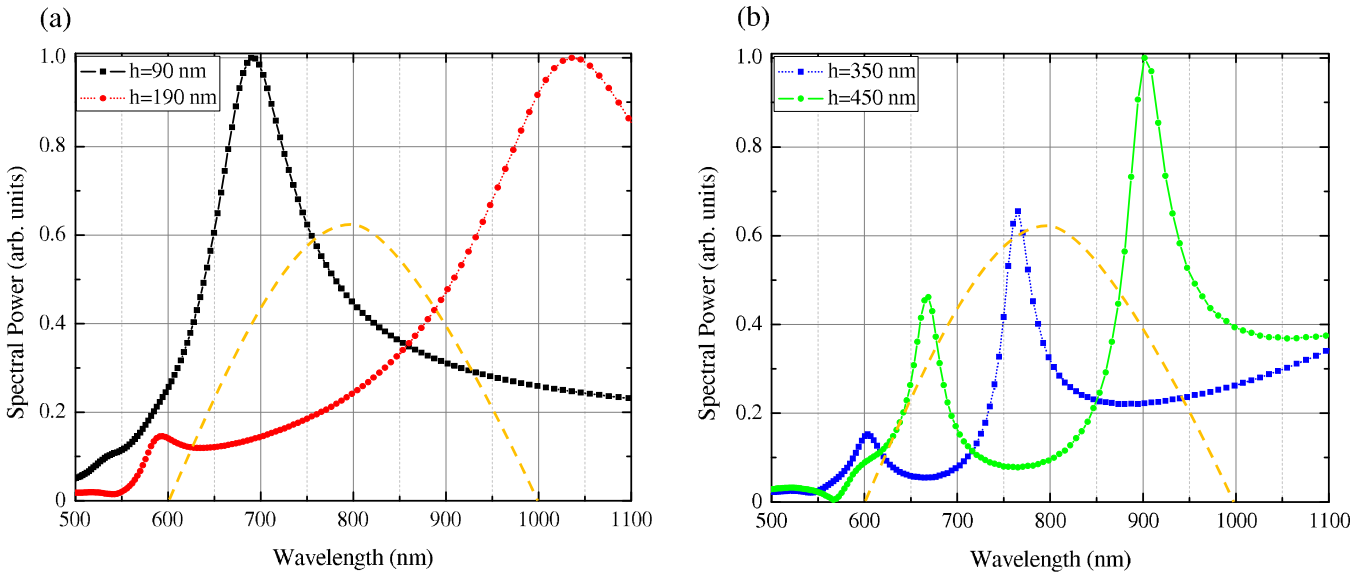

FIG. 2. Plasmonic resonance characteristics for given geometrical parameters of nanoantenna. The wavelength of incident light is swept from 500 to 1100 nm. The spectral power is calculated from the electric field at the center of bow-tie gap and every data is normalized by maximum spectral power at a given wavelength range. The resultant resonance characteristics are shown in graphs for different bow-tie heights of 90 nm [black squares in Fig. 2(a)], 190 nm [red circles in Fig. 2(a)], 350 nm [blue squares in Fig. 2(b)], and 450 nm [green circles in Fig. 2(b)]. The orange dashed line in each panel represents the original spectrum of 5 fs pulse to compare the spectral overlapping with the plasmonic resonance spectrum of each nanoantenna.

for $h = 90$ nm and $h = 190$ nm are ∼700 and ∼1000 nm, respectively, which bounds the degree of blue- and redshift, respectively, of the driving laser that can be achieved by these two geometries. This is indeed confirmed by Fig. 1(b), where all central wavelengths fall within the 700–1000 nm range. Hence, it is clear that for very short pulses (but not longer pulses), the spectral characteristics of the near field are dominated by the geometry of the nanostructure. This can be understood by considering that, when the spectral components of an incident pulse are far from the intrinsic resonant wavelength, each spectral component experiences more or less uniform enhancement. However, when the spectral distribution of an incident pulse overlaps with the plasmonic resonance wavelength, there is a dramatic difference of field enhancement between spectral components near to and far from the plasmonic resonant wavelength of a nanoantenna. This brings about a shift of the λ of the resultant near field, which is much more pronounced for broadband pulses whose spectra contain a significant component of the resonant wavelength. In addition, for a geometry where a double resonance exists, such as $h = 450$ nm, shown in Fig. 2(b), it is possible to create a two-color ultrashort pulse at the nanoscale. Hence, for a broadband pulse excitation, a nanoantenna acts like a transfer function of a pump source, which provide us with the ability to control the spectrum.

Figure 3(a) shows the height-dependent shift of λ under different optical pulse widths of 5, 10, and 30 fs (in the presence of a double resonance, the higher peak was selected as the λ). The corresponding spectra for 5 and 10 fs pulses are shown in Figs. 3(b) and 3(c), respectively. In the case of 30 fs pulse excitation, no significant shift of λ was observed, consistent with results in [6,18], even though the height of the nanoantenna was varied from 60 to 450 nm. In contrast, a significant oscillation of λ was observed for a 5-fs pulse excitation, further confirming the sensitive dependence on nanoantenna geometry. For $h > 210$ nm, the resonance wavelength gradually decreases again, showing a continuous variation from a redshifted region to a blueshifted one and vice versa. When the bow-tie height exceeds ∼300 nm, two distinct peaks starts to appear, as a result of a double resonance, and the separation of two peaks gets larger as the bow-tie height is further increased.

The double resonance characteristic that we found for certain geometries [see Fig. 2(b)], leads to a two-color ultrafast plasmonic near field when the nanostructure interacts with a few-cycle laser pulse [see Fig. 3(b), green curve]. It has previously been shown that the proper mixing of two colors results in an asymmetry of the electric field that is favorable to the generation of an isolated attosecond pulse [20–26]. In particular, the mixture of different color and amplitude fields can result in a larger difference in the field amplitude among neighboring cycles than in a single color field, which, in turn, favors the generation of shorter isolated attosecond pulses. Hence, the mixing of 6 fs FWHM, 800 nm laser with 21.3 fs FWHM, 400 nm [21] or 64 fs FWHM, 2400 nm [21] has been theoretically shown to generate a sub-100 as pulse. In addition, Merdji and colleagues showed that the mixing of detuned second harmonic of an 800 nm, 40 fs FWHM pulse (the fundamental field) can generate sub-100 as pulse more efficiently than the mixing of the second harmonic [26]. A subsequent work investigated the mixing of an 800 nm few-tens fs laser with a fs laser at 1.2 to 2.4 μm [20], showing the possibility of 100–300 as isolated attosecond pulse.

To investigate whether the two-color field generated in the bow-tie gap can be favorable for the generation of isolated attosecond pulses, we have simulated the HHG spectra using

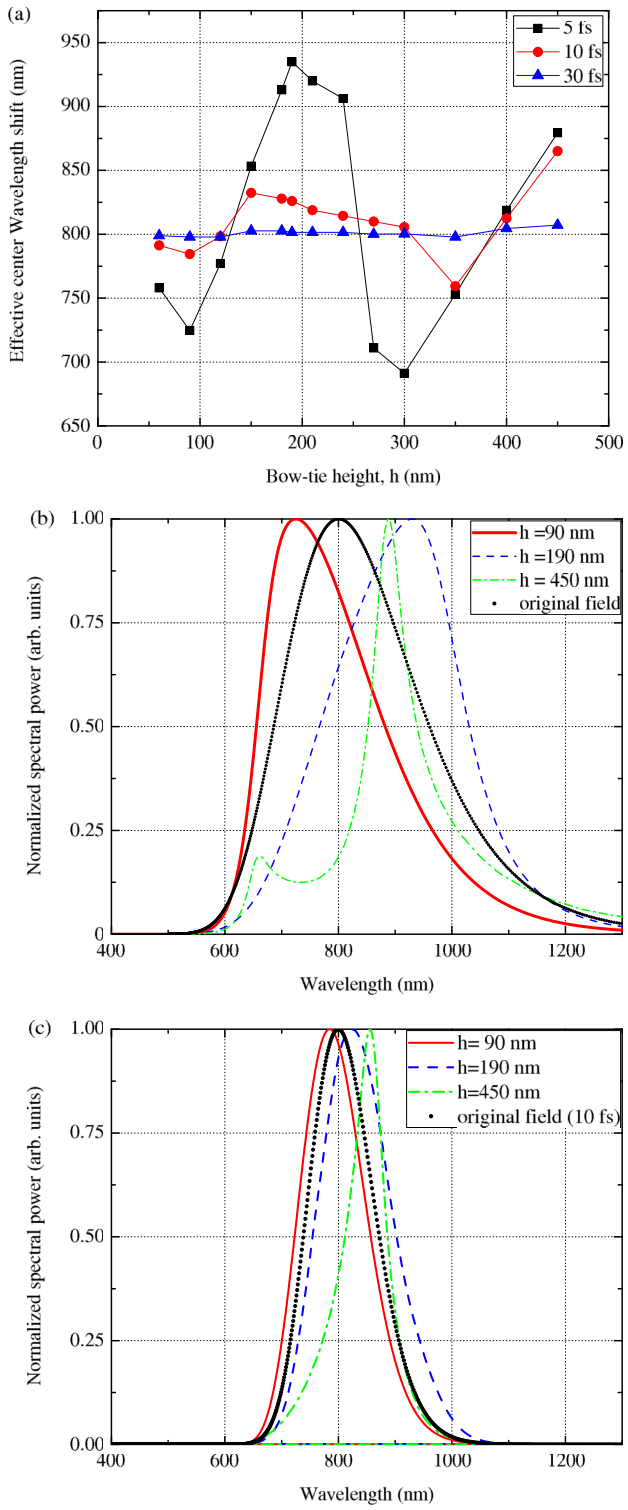

FIG. 3. (a) Effective center wavelength shift for the variation of bow-tie height at three different pulse widths. 5 fs (black squares), 10 fs (red circles), and 30 fs (blue triangles). (b) Resultant spectra of near field for three different bow-tie heights, namely, 90 nm (red solid line), 190 nm (blue dashed line), and 450 nm (green dot-dashed line) for 5 fs pulse excitation. (c) Same as (b), but for 10 fs pulse excitation. In both panels the original field is shown with black circles.

the time-dependent Schrödinger equation (TDSE). Since the dynamics of an atomic electron in a linearly polarized strong laser field mainly takes place along the direction of the field, we restrict our TDSE simulations to one dimension (1D-TDSE):

$$i\frac{\partial\Psi(x,t)}{\partial t} = \left[-\frac{1}{2}\frac{\partial}{\partial x^2} + V_{\text{atom}}(x) + V_{\text{laser}}(x,t)\right]\Psi(x,t). \quad (1)$$

To model the atom, we employ the widely used quasi-Coulomb or soft-core potential [27], given by $V_{\text{atom}}(x) = -Z/\sqrt{x^2+\alpha(Z)}$, where Z is the atomic number and $\alpha(Z) = 2/Z^2$ is chosen to satisfy the ground state energy of the Coulomb potential: $-I_p = -Z^2/2$. In all the simulations, we used the parameters for a hydrogen atom, although any other atom could be used. In Eq. (1), $V_{\text{laser}}(x,t) = -E(t)x$, where the laser electric field $E(t)$ was obtained from the FDTD simulations including all the time-dependent spectral properties.

Equation (1) above was solved numerically by using the Crank-Nicolson scheme and in order to avoid spurious reflections from the boundaries, at each time step, the total electronic wave function was multiplied by a mask function. Once the time-propagated electron wave function of the system from the 1D-TDSE was found, we calculated the harmonic spectrum by Fourier transforming the dipole acceleration of the active electron:

$$D(\omega) = \left|\frac{1}{\tau}\frac{1}{\omega^2}\int_{-\infty}^{\infty} dt\, e^{-i\omega t}a(t)\right|^2, \quad (2)$$

where $a(t) = d^2\langle\Psi|x|\Psi\rangle/dt^2$ and τ is the time duration of the laser pulse (for more details see, e.g., [13]).

The resulting HHG spectrum is plotted in Fig. 4(a) for the case of $h = 450$ nm, where a double resonance exists in the nanoantenna, leading to a two-color near field when excited by a few-cycle IR pulse. For comparison, the HHG spectrum created by the driving few-cycle laser pulse only (without the presence of the nanoantenna) is displayed in Fig. 4(b). We have employed an *enhanced* field intensity of 8×10^{13} W/cm^2 in both cases and the temporal evolution of the field can be seen as insets in the HHG spectra of Figs. 4(a) and 4(b). The input laser pulse has a FWHM pulse duration of 5 fs and from the inset of Fig. 4(a) we can observe the appreciable modifications experienced by this pulse as a consequence of the interaction with the plasmonic nanostructure. According to the semiclassical model [28], the HHG cutoff at this intensity and for an H atom is equal to the 19th harmonic, for a $\lambda = 800$ nm. As can be seen, our model is able to reproduce the limit in the HHG spectrum [Fig. 4(b)]. In a typical gas-jet experiment, the harmonic coherence length should be taken into account, in order to assess if phase-matching effects are important (see, e.g., [29] for details). In our proposed setup, however, the emission of radiation is confined to a very tiny region—each emitter acts as a pointlike source of nanometric dimensions that radiates high harmonics with a broad angle distribution, and consequently the coherent radiation collectively observed from the array of elements maintains high coherence in both spatial and temporal terms. According to this behavior no phase-matching condition consideration is required, but a multiscale study may be needed in order to confirm this phenomenological fact (see. e.g.. [30,31] for more details). As shown in Fig. 4(a), the use of the plasmonic field led to a broader spectrum and to the

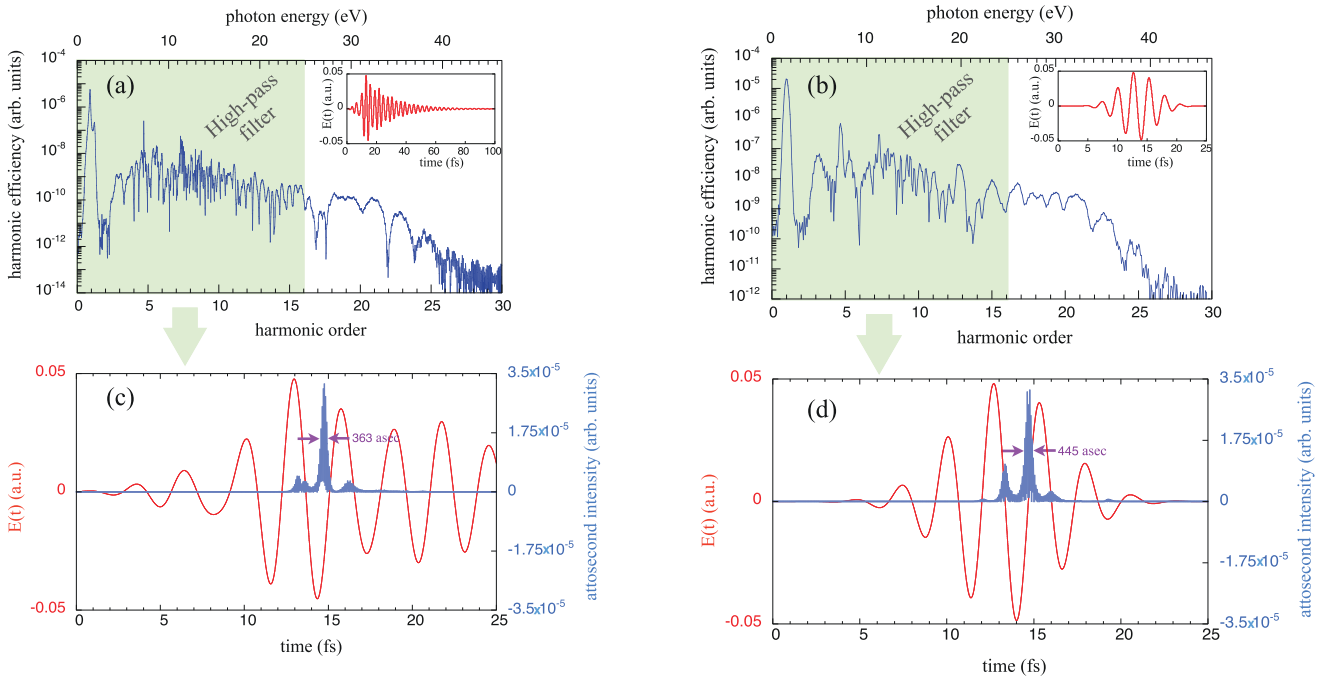

FIG. 4. Calculated high-order harmonic spectrum and attosecond pulse for 450 nm height bow-tie nanoantenna for extracted plasmonic field (a) and (c) and for 5 fs original excitation pulse (b) and (d). The plasmonic and original fields vs. time are shown as an inset of each figure (a) and (b), respectively. From the same spectral high-pass filtering at the cutoff of 16th harmonic (25 eV), isolated attosecond pulses are generated. Due to the spectral modification, a shorter isolated attosecond pulse is attainable from the plasmonic field case.

extension of the HHG cutoff. The higher HHG cutoff can be explained by noting that the λ of the plasmonic near field is redshifted with respect to the driving laser [see Fig. 3(b), green curve].

By applying an inverse Fourier transform to the HHG spectra, the time domain is recovered and subfemtosecond structures are observed by utilizing an adequate set of XUV filters from the original HHG spectra [Figs. 4(c) and 4(d)]. In our case, we employed a high-pass filter blocking the radiation below the 16th harmonic (25 eV). In order to show when an attosecond pulse is generated and its FWHM duration, we have superimposed these subfemtosecond structures on the temporal shape of the laser pulse. By comparison between Figs. 4(c) and 4(d) we note that the laser pulse modified by the plasmonic structure supports shorter attosecond pulses with a much better contrast between the main central peak and the side band peaks. It is important to note that in spite of the fact that the interaction with the plasmonic nanostructure increases the pulse duration [see Fig. 4(a)], an isolated attosecond pulse is still obtained, narrower and cleaner than in the case of the original few-cycle pulse. This is likely due to two-color mixing coming from the double resonance feature. Due to the fact that the pulse gets longer after interacting with the plasmonic structure, the role of the carrier-envelope phase (CEP) and pulse chirp in the attosecond pulse generation appears to be less relevant. To test the importance of the CEP and the influence of the pulse chirp, we have conducted a set of simulations for different CEP values and varying the degree of a second-order chirp (not shown). We have confirmed the resultant HHG spectra show similar structure and a comparable cutoff for the different CEP values. Furthermore, the response of the surface-plasmon resonance to each single wavelength (frequency) is not correlated with other frequency components. Because the pulse chirp is the relative phase change in each wavelength component, this phase modification does not affect the spectral properties of the plasmonic field enhancement. Therefore, the plasmonic resonance for broadband excitation is a linear superposition of each plasmonic resonance field by single wavelength (frequency) excitation. In light of this intrinsic property of the plasmonic resonance, the spectral modification (shift of carrier wavelength) is not affected by the change of CEP and degree of chirp. We have also confirmed this behavior by computing the spectral properties of the nanoantenna as a function of different CEP values and degree of chirp.

In conclusion, we show that the variation of nanostructure geometry offers control over the nonlinear response excited by a few-cycle laser pulse that is considerably different from the bulk. In particular, the bow-tie nanoantenna was able to modify the frequency (wavelength) components of the incident pulse by a substantial amount (on the order of 100 nm), shifting the signal centered at ω_1 (λ_1) by an amount $\Delta\omega$ ($\Delta\lambda$) into a new frequency band centered at ω_2 (λ_2). We demonstrate that in order for this to happen two conditions have to be satisfied: (i) a mismatch between the intrinsic resonance of the plasmonic mode and the central frequency of the laser, and (ii) the laser pulse has to be sufficiently broadband to have significant overlap with the resonant plasmonic mode. Our findings are consistent with the measurements performed by Dombi and colleagues [12], which found a significant shift in λ with variation of geometry when a broadband white light source shines on a nanostructure. Condition (ii) explains why

such a dramatic, geometry-dependent, modification in the time dependence of the near field has not been previously observed for nanostructures subjected to a laser pulse. In particular, prior experiments, which investigated the near field, have used laser pulses which were at least 10 fs or longer [6,18], leading to only minor shifts of λ. The bow-tie dimensions can be engineered to meet the requirements of resonance according to the spectral bandwidth of the incident pulse and vice versa, leading to versatile and tunable sources of radiation at a nanoscale. The tunability in the bandwidth of the output spectrum and the creation of a second color (due to a double resonance) can be used to achieve shorter and cleaner isolated attosecond pulses via spectrally tailored plasmonic fields without special laser techniques. Hence, our results show how few-cycle pulses and tailored nanostructure geometries can be used for new applications in nonlinear light generation and pulse shaping at a nanoscale. Although the improvement in the attosecond pulse time duration is not striking, our scheme also supports other nonlinear harmonic generation, such as second and third harmonic generation. In addition, the attosecond pulse generation at megahertz repetition rate is clearly a significant achievement and is related to the amplification of the incoming pulse due to the plasmonic nanoantenna.

This work was supported in part by the Global Research Laboratory Program (Grant No. 2009-00439), Max Planck POSTECH / KOREA Research Initiative Program (Grant No. 2011-0031558) and Basic Science Research Program (NRF-2013R1A1A2004932) through the National Research Foundation of Korea (NRF) funded by Ministry of Science, ICT & Future Planning (Republic of Korea). A.S.L. acknowledges the support of the Max Planck Center for Attosecond Science (MPC-AS). J.A.P.-H. acknowledges the Laserlab-Europe (Grant No. EU FP7 284464) and the Spanish Ministerio de Economía y Competitividad (FURIAM Project No. FIS2013-47741-R). This research was supported by the Infrastructure and Transportation Technology Promotion Research Program (14CTAP-C077584-01) funded by Ministry of Land, Infrastructure and Transport of Korean government (Republic of Korea). Y.-J. Kim acknowledges support from the Singapore National Research Foundation (Grant No. NRF-NRFF2015-02) (Singapore).

[1] W. L. Barnes, A. Dereux, and T. W. Ebbesen, Surface plasmon subwavelength optics, Nature (London) **424**, 824 (2003).

[2] M. Kauranen and A. V. Zayats, Nonlinear plasmonics, Nat. Photonics **6**, 737 (2012).

[3] M. I. Stockman, Nanoplasmonic sensing and detection, Science **348**, 287 (2015).

[4] M. I. Stockman, Nanofocusing of Optical Energy in Tapered Plasmonic Waveguides, Phys. Rev. Lett. **93**, 137404 (2004).

[5] T. Hanke, J. Cesar, V. Knittel, A. Trügler U. Hohenester, A. Leitenstorfer, and R. Bratschitsch, Tailoring spatiotemporal light confinement in single plasmonic nanoantennas, Nano Lett. **12**, 992 (2012).

[6] B. Metzger, M. Hentschel, T. Schumacher, M. Lippitz, X. Ye, C. B. Murray, B. Knabe, K. Buse, and H. Giessen, Doubling the efficiency of third harmonic generation by positioning ITO nanocrystals into the hot-spot of plasmonic gap-antennas, Nano Lett. **14**, 2867 (2014).

[7] H. Kollmann, X. Piao, M. Esmann, S. F. Becker, D. Hou, C. Huynh, L.-O. Kautschor, G. Bösker, H. Vieker, A. Beyer, A. Gölzhäuser, N. Park, R. Vogelgesang, M. Silies, and C. Lienau, Toward plasmonics with nanometer precision: Nonlinear optics of helium-ion milled gold nanoantennas, Nano Lett. **14**, 4778 (2014).

[8] P. L. Stiles, J. A. Dieringer, N. L. Shah, and R. P. Van Duyne, Surface-enhanced Raman spectroscopy, Annu. Rev. Anal. Chem. **1**, 601 (2008).

[9] M. S. Tame, K. R. McEnery, Ş. K. Özdemir, J. Lee, S. A. Maier, and M. S. Kim, Quantum plasmonics, Nat. Phys. **9**, 329 (2013).

[10] J. A. Schuller *et al.*, Plasmonics for extreme light concentration and manipulation, Nat. Mater. **9**, 193 (2010).

[11] K. F. MacDonald, Z. L. Sàmson, M. I. Stockman, and N. I. Zheludev, Ultrafast active plasmonics, Nat. Photonics **3**, 55 (2009).

[12] P. Dombi, A. Hörl, P. Rácz, I. Márton, A. Trügler, J. R. Krenn, and U. Hohenester, Ultrafast strong-field photoemission from plasmonic nanoparticles, Nano Lett. **13**, 674 (2013).

[13] M. F. Ciappina, J. Biegert, R. Quidant, and M. Lewenstein, High-order harmonic generation from inhomogeneous fields, Phys. Rev. A **85**, 033828 (2012).

[14] M. F. Ciappina, Srdjan S. Aćimović, T. Shaaran, J. Biegert, R. Quidant, and M. Lewenstein, Enhancement of high harmonic generation by confining electron motion in plasmonic nanostructures, Opt. Express **20**, 26261 (2012).

[15] J. A. Pérez-Hernández, M. F. Ciappina, M. Lewenstein, L. Roso, and A. Zaïr, Beyond Carbon *K*-edge Harmonic Emission Using Spatial and Temporal Synthesized Laser Fields, Phys. Rev. Lett. **110**, 053001 (2013).

[16] P. J. Schuck, D. P. Fromm, A. Sundaramurthy, G. S. Kino, and W. E. Moerner, Improving the Mismatch between Light and Nanoscale Objects with Gold Bowtie Nanoantennas, Phys. Rev. Lett. **94**, 017402 (2005).

[17] T. Hanke, G. Krauss, D. Träutlein, B. Wild, R. Bratschitsch, and A. Leitenstorfer, Efficient Nonlinear Light Emission of Single Gold Optical Antennas Driven by Few-Cycle Near-Infrared Pulses, Phys. Rev. Lett. **103**, 257404 (2009).

[18] H. Aouani, M. Rahmani, M. Navarro-Cía, and S. A. Maier, Third-harmonic-upconversion enhancement from a single semiconductor nanoparticle coupled to a plasmonic antenna, Nat. Nanotechnol. **9**, 290 (2014).

[19] E. D. Palik, *Handbook of Optical Constants of Solids* (Academic, New York, 1997).

[20] B. Kim, J. Ahn, Y. Yu, Y. Cheng, Z. Xu, and D. Kim, Optimization of multi-cycle two-color laser fields for the generation of an isolated attosecond pulse, Opt. Express **16**, 10331 (2008).

[21] Z. Zeng, Y. Cheng, X. Song, R. Li, and Z. Xu, Generation of an Extreme Ultraviolet Supercontinuum in a Two-Color Laser Field, Phys. Rev. Lett. **98**, 203901 (2007).

[22] X. Song, Z. Zeng, Y. Fu, B. Cai, R. Li, Y. Cheng, and Z. Xu, Quantum path control in few-optical-cycle regime, Phys. Rev. A **76**, 043830 (2007).

[23] T. Pfeifer, L. Gallmann, M. J. Abel, P. M. Nagel, D. M. Neumark, and S. R. Leone, Heterodyne Mixing of Laser Fields for Temporal Gating of High-Order Harmonic Generation, Phys. Rev. Lett. **97**, 163901 (2006).

[24] Y. Huo, Z. Zeng, R. Li, and Z. Xu, Single attosecond pulse generation using two-color polarized time-gating technique, Opt. Express **13**, 9897 (2005).

[25] Y. Yu, X. Song, Y. Fu, R. Li, Y. Cheng, and Z. Xu, Theoretical investigation of single attosecond pulse generation in an orthogonally polarized two-color laser field, Opt. Express **16**, 686 (2008).

[26] H. Merdji, T. Auguste, W. Boutu, J.-Pascal Caumes, B. Carré, T. Pfeifer, A. Jullien, D. M. Neumark, and S. R. Leone, Isolated attosecond pulses using a detuned second-harmonic field, Opt. Lett. **32**, 3134 (2007).

[27] Q. Su and J. H. Eberly, Model atom for multiphoton physics, Phys. Rev. A **44**, 5997 (1991).

[28] M. Lewenstein, P. Balcou, M. Y. Ivanov, A. L'Huillier, and P. B. Corkum, Theory of high-harmonic generation by low-frequency laser fields, Phys. Rev. A **49**, 2117 (1994).

[29] C. Altucci, R. Bruzzese, C. de Lisio, M. Nisoli, E. Priori, S. Stagira, M. Pascolini, L. Poletto, P. Villoresi, V. Tosa, and K. Midorikawa, Phase-matching analysis of high-order harmonics generated by truncated Bessel beams in the sub-10-fs regime, Phys. Rev. A **68**, 033806 (2003).

[30] S. Kim, J. Jin, Y.-J. Kim, I.-Y. Park, Y. Kim, and S.-W. Kim, High-harmonic generation by resonant plasmon field enhancement, Nature (London) **453**, 757 (2008).

[31] I.-Y. Park, S. Kim, J. Choi, D.-H. Lee, Y.-J. Kim, M. F. Kling, M. I. Stockman, and S.-W. Kim, Plasmonic generation of ultrashort extreme-ultraviolet light pulses, Nat. Photonics **5**, 677 (2011).